



# Pb-based metal organic framework as substrate: Chemical vapor generation-visual/smartphone colorimetric analytical system for sensitive and selective detection of sulfide ion in water and beers

Jihong Chen<sup>a</sup>, Qian Yao<sup>b</sup>, Xiaoyu Dong<sup>a</sup>, Jiayuan Tang<sup>a</sup>, Shu Zhang<sup>a</sup>, Yuyao Ji<sup>a,\*</sup>, Zhirong Zou<sup>a,b,\*</sup>

<sup>a</sup> Key Laboratory of the Evaluation and Monitoring of Southwest Land Resources (Ministry of Education), College of Chemistry and Material Science, Sichuan Normal University, Chengdu, Sichuan 610068, China

<sup>b</sup> School of Chemistry and Chemical Engineering, Key Laboratory of Low-cost Rural Environmental Treatment Technology, Special Polymer Materials for Automobile Key Laboratory of Sichuan Province, Sichuan Institute of Arts and Science, Dazhou, Sichuan 635000, China

## ARTICLE INFO

### Keywords:

Sulfide ion ( $S^{2-}$ )  
Chemical vapor generation  
Colorimetric  
Metal organic framework

## ABSTRACT

A visual/smartphone colorimetric system was developed for the sensitive and selective detection of sulfide ion ( $S^{2-}$ ) using chemical vapor generation (CVG) as a gaseous sampling technique.  $S^{2-}$  in samples were converted into  $H_2S$  after the addition of  $H_2SO_4$ , which separated from the solution during CVG process, ensuring high efficiency of vapor generation (sensitivity) and eliminated interferences (selectivity). The  $H_2S$  was subsequently reacted with Pb-BTC and PbS was thus formed, causing the test paper turned to black. It was utilized for the detection of  $S^{2-}$  by visual/smartphone colorimetric system. Detectable limits of 0.05  $\mu\text{g/mL}$  and 0.2  $\mu\text{g/mL}$  were obtained under smartphone mode and visual mode, respectively. Furthermore, this colorimetric system was successfully used for the analysis of  $S^{2-}$  in several beer samples and water samples, with recoveries ranging 97%–111%. This system represents a potential miniaturized, easy used and high-effective method for rapid and on-site detection of  $S^{2-}$ .

## 1. Introduction

As a hazardous contaminant, sulfide ( $S^{2-}$ ) ion is commonly found in industrial processes and biological systems, prevalent in industrialized wastewater from oil refineries, food factories and tanneries (Liu et al., 2019; Rajamanikandan & Ilanchelian, 2022). Excessive sulfide accumulation poses environmental and biological hazards, causing irritation to respiratory mucous membranes and skin sensitization upon prolonged exposure (Yin et al., 2022). Furthermore, serious health implications such as Down's syndrome, Alzheimer's disease, cirrhosis of the livers and diabetes mellitus have been associated with sulfide exposure (Chen et al., 2024). Consequently, the World Health Organization (WHO) requires that the level of  $S^{2-}$  in water should not exceed 15  $\mu\text{M}$  (0.5  $\mu\text{g/mL}$ ) (So et al., 2019), underscoring the importance of monitoring  $S^{2-}$  content in environmental water.

Various methods are available for  $S^{2-}$  detection, including gas chromatography (Zhang et al., 2014), surface-enhanced Raman

scattering (Li et al., 2015), electrochemical assays (Chen et al., 2021; Hall & Schoenfisch, 2018), fluorescence spectroscopy (Buragohain & Biswas, 2016; Wang et al., 2018) and ultraviolet-visible spectroscopy (Tang et al., 2019). However, these methods often require bulky instruments and complicated operations, restricting instruments to laboratory use only. As a consequent, there is a critical need for a rapid on-site detection method.

Chemical vapor generation (CVG), including hydride generation and photochemical vapor generation etc., as a mature gaseous sample introduction technique, offers benefits such as high efficiency of sample introduction and efficient sample matrix separation etc. (Campanella & D'Ulivo, 2024; Hu et al., 2022). Nowadays, CVG has been combined with atomic spectrometry and applied to the determination of elements (Li et al., 2023; Wu et al., 2010; Zou et al., 2019; Zou et al., 2020). Colorimetric methods have attracted widespread attention due to its advantages of low cost, ease of operation and visualization (Tian et al., 2024). The combination of colorimetry and chemical vapor generation has the

\* Corresponding authors at: Key Laboratory of the Evaluation and Monitoring of Southwest Land Resources (Ministry of Education), College of Chemistry and Material Science, Sichuan Normal University, Chengdu, Sichuan 610068, China.

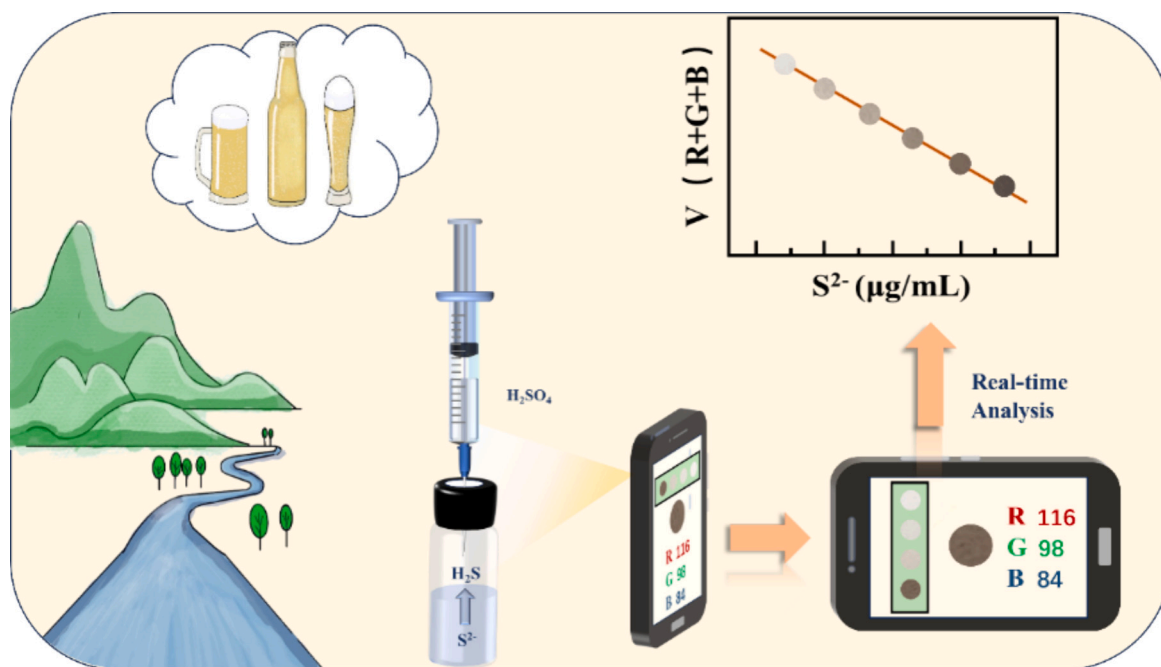
E-mail addresses: [yyji@sicnu.edu.cn](mailto:yyji@sicnu.edu.cn) (Y. Ji), [zouzhirong@sicnu.edu.cn](mailto:zouzhirong@sicnu.edu.cn) (Z. Zou).

<https://doi.org/10.1016/j.fochx.2024.101767>

Received 9 June 2024; Received in revised form 8 August 2024; Accepted 22 August 2024

Available online 24 August 2024

2590-1575/© 2024 The Author(s). Published by Elsevier Ltd. This is an open access article under the CC BY-NC license (<http://creativecommons.org/licenses/by-nc/4.0/>).



Scheme. 1. Schematic diagram of the proposed CVG-colorimetric system.

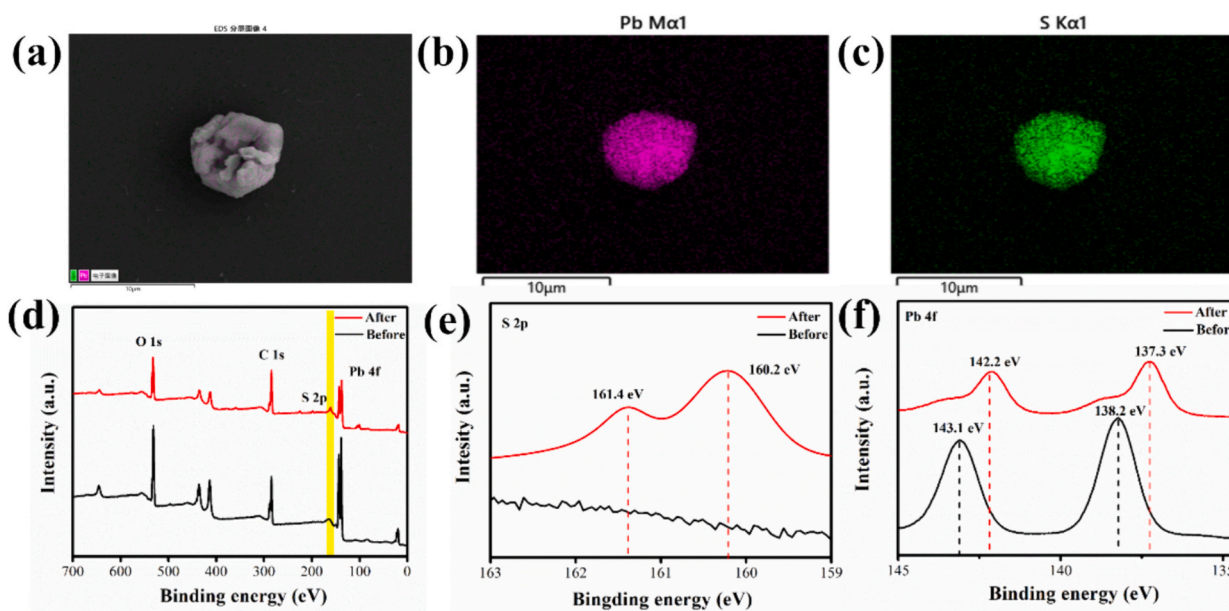


Fig. 1. Energy-dispersive spectroscopy mapping of Pb-BTC (a-c), XPS data of Pb-BTC: full XPS spectra (d), S (e) and Pb (f).

potential to produce superior results. Currently, this conjunction is employed for detection of various analytes (Hu et al., 2019), including antimony (Tolessa et al., 2018), selenium (Xiong et al., 2019), nickel (Yuan et al., 2022), zinc (Huang et al., 2018) and arsenic (Jiang et al., 2023; Zou et al., 2023). Notably, CVG-based colorimetric systems also can be utilized for  $S^{2-}$  analysis. Hou et al. proposed a fluorescence sensor for detection of  $S^{2-}$ .  $S^{2-}$  was converted into gaseous  $H_2S$  upon addition of HCl, and  $H_2S$  quenched the paper-based fluorescence of CdTe quantum dots through a gas-solid reaction (Pan et al., 2021). Additionally, Zheng et al. proposed a paper-based ratiometric fluorescent sensor for field analysis of  $S^{2-}$ , constructing by the inner filter effect of CdS quantum dots toward carbon dots (C-dots).  $S^{2-}$  was converted to  $H_2S$  after the addition of  $H_2SO_4$ , and CdS quantum dots were in-situ formed. CdS was acted as an energy acceptor to quench the emission of C-dots.

The increasing concentration of  $S^{2-}$  lead to a ratiometric fluorescence change to yellow from blue (Lin et al., 2023). Metal organic frameworks (MOFs) are porous materials with a wide range of applications, which are formed by the coordination of central metal ions and organic ligands, and take advantages of high porosity, large specific surface area and good stability etc. (Li et al., 2020; Yang et al., 2022; Yuan et al., 2023; Zhang et al., 2023). Thanks to the above-mentioned advantages, MOFs can preconcentrate the analyte gas, which not only improves the sensitivity and selectivity, but also accelerates the reaction rate. Therefore, MOFs are potential colorimetric substrates for elemental analysis. However, to date, lead-based MOF has not been reported as a substrate for colorimetric analysis of  $S^{2-}$ .

In this work, a lead-containing metal organic framework (Pb-BTC) was prepared and served as a substrate for  $S^{2-}$  analysis by chemical

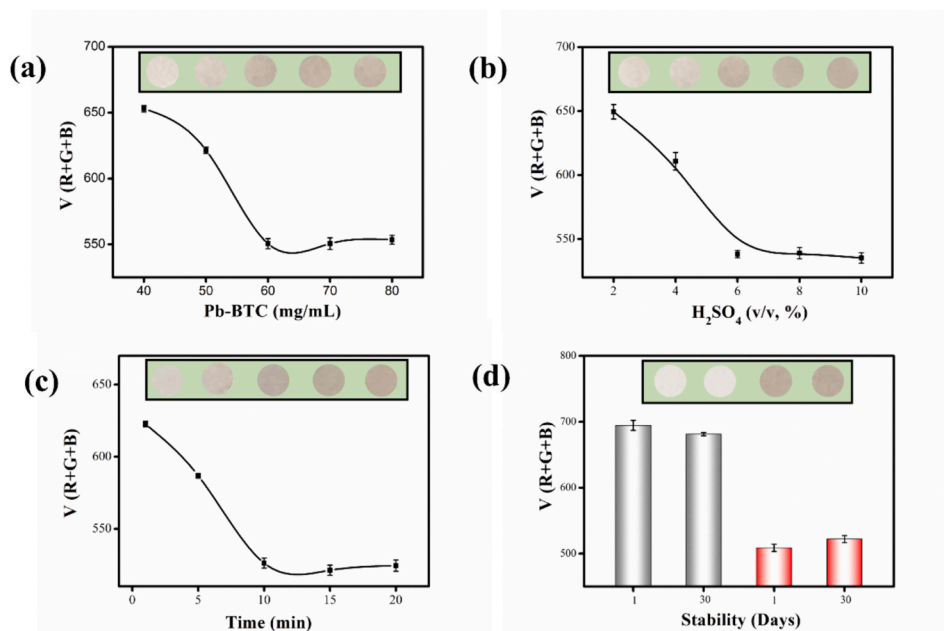


Fig. 2. (a) Effect of Pb-BTC concentration, (b) effect of  $H_2SO_4$  concentration, (c) effect of reaction time and (d) stability of Pb-BTC (new test paper: 1 day; old test paper: 30 days).

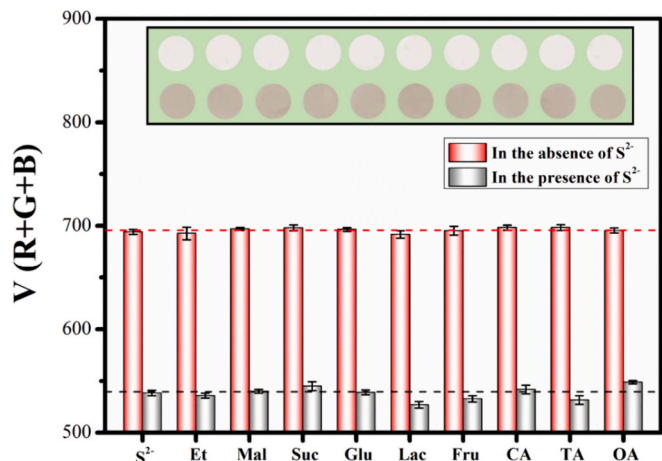


Fig. 3. Interferences for  $S^{2-}$  detection. (Et: ethanol; Mal: maltose; Suc: sucrose; Glu: glucose; Lac: lactose; Fru: fructose; CA: citric acid; TA: tartaric acid; OA: oxalic acid).

vapor generation-colorimetric system.  $S^{2-}$  was transformed to  $H_2S$  gas after  $H_2SO_4$  was added.  $H_2S$  reacted with Pb-BTC, PbS was subsequently formed on the surface of Pb-BTC, turning the Pb-BTC into black from white, this color variance was finally readout by visual method and smartphone RGB readout method. Several beer samples and water samples were further detected by this colorimetric system, with recoveries of 97%–111%. Detectable limits of 0.05  $\mu\text{g/mL}$  and 0.2  $\mu\text{g/mL}$  can be identified by a smartphone and naked-eye, respectively. This colorimetric method is a promising portable analytical system for rapid and field analysis of  $S^{2-}$ .

## 2. Experimental section

### 2.1. Reagents

In this study, all reagents were used without purification and were commercially available. 18.25 M $\Omega$  cm deionized water (DIW) were used for solutions preparation.  $Pb(NO_3)_2$ , trimesic acid ( $H_3BTC$ ), NaOH,  $H_2SO_4$ ,  $Na_2SO_4$ ,  $K_2SO_4$ , NaF, NaCl, NaBr, KI,  $Na_2CO_3$ ,  $Na_3PO_4 \cdot 12H_2O$ ,  $NaNO_3$ ,  $CH_3COONa$ , ethanol, fructose, lactose, maltose, sucrose, glucose, tartaric acid, oxalic acid and citric acid were purchased from Kelong Chemical Reagents Co. Ltd. (Chengdu, China). The  $Na_2S$

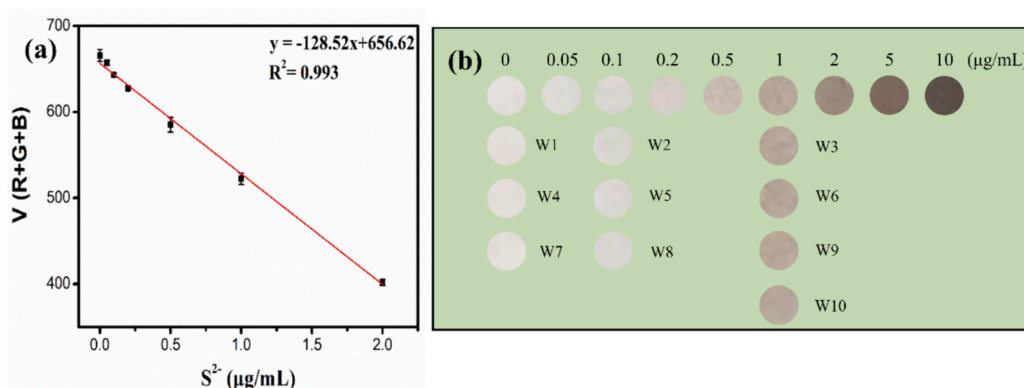















Fig. 4. (a) Calibration curve of smartphone readout method. (b) Standard cards of visual method and water samples analysis.

**Table 1**  
Analytical results of  $S^{2-}$  in water samples and beer samples by the proposed method.

Samples	Certified value ( $\mu\text{g}/\text{mL}$ )	$S^{2-}$ added ( $\mu\text{g}/\text{mL}$ )	Detected by RGB method ( $\mu\text{g}/\text{mL}$ )	Naked-eye	Recovery (%)
Qinglong Lake water (W1)	–	–	ND	–	–
(W2)	–	0.1	$0.106 \pm 0.018$		106
(W3)	–	1	$1.108 \pm 0.044$		111
East Lake water (W4)	–	–	ND	–	–
(W5)	–	0.1	$0.108 \pm 0.012$		108
(W6)	–	1	$1.094 \pm 0.032$		109
Tap water (W7)	–	–	ND	–	–
(W8)	–	0.1	$0.105 \pm 0.009$		105
(W9)	–	1	$1.080 \pm 0.073$		108
BWZ6676-2016C* (W10)	1	–	$1.018 \pm 0.030$		102
Beer sample 1 (B1)	–	–	ND	–	–
(B2)	–	0.1	$0.099 \pm 0.017$		99
(B3)	–	1	$1.087 \pm 0.024$		109
Beer sample 2 (B4)	–	–	ND	–	–
(B5)	–	0.1	$0.097 \pm 0.014$		97
(B6)	–	1	$0.996 \pm 0.090$		99
Beer sample 3 (B7)	–	–	ND	–	–
(B8)	–	0.1	$0.103 \pm 0.023$		103
(B9)	–	1	$1.042 \pm 0.026$		104

ND: not detected. \* BWZ6676-2016C certified value: 2.06  $\mu\text{g}/\text{mL}$ , diluted to 1  $\mu\text{g}/\text{mL}$  (W10) before analysis.

standard solution (1000  $\mu\text{g}/\text{mL}$ ) and Certified Reference Material (CRM) of water (BWZ6676-2016C) were purchased from Beijing Century Aoke Biotechnology. Chromatography paper and filter papers were obtained from Whatman U.K. Beer samples were acquired from local supermarket, tap water was collected from Sichuan Normal University, and lake water samples were collected from Qinglong Lake Park and East Lake Park (Chengdu), respectively.

## 2.2. Characterizations

Deionized water (DIW, 18.25  $\text{M}\Omega$  cm) was obtained from a water purification system. The X-ray photoelectron spectroscopy (XPS) data and scanning electron microscope (SEM) images were provided by an ESCALABMK II X-ray photoelectron spectrometer and a Quanta 250

SEM (FEI Instrument Co. USA), respectively. X-ray diffraction (XRD) data was obtained using a RigakuD/MAX 2550 diffractometer. The Fourier transform infrared spectroscopy (FTIR) data was obtained from Bruker Optics VERTEX 70.

## 2.3. Synthesis of Pb-BTC

The Pb-BTC ( $[\text{Pb}_2(1,3,5\text{-HBTC})_2(\text{H}_2\text{O})_4]\cdot\text{H}_2\text{O}$ ) was prepared following a previously reported procedure with some modifications (Zhang et al., 2017). Initially, dissolve 0.189 g trimesic acid ( $\text{H}_3\text{BTC}$ ) in 90 mL  $\text{H}_2\text{O}$  using a high-density ultrasonic cleaner, yielding solution A. Subsequently, 0.298 g  $\text{Pb}(\text{NO}_3)_2$  was dissolved in 10 mL of  $\text{H}_2\text{O}$  to form solution B. Solution B was then added to solution A, followed by ultrasonication for 30 min at room temperature. The synthesized Pb-BTC was washed several times with ethanol and then dried in an oven at 60  $^\circ\text{C}$ . XRD spectrum of Pb-BTC was coincided with its simulated data (Fig. S1, CCDC: 722465) (Sadeghzadeh & Morsali, 2010), confirming the successful synthesis of Pb-BTC. The FTIR spectrum of synthesized Pb-BTC was presented in Fig. S2, it was matched well with the previous literature (Baskoro et al., 2021), further demonstrating the successful synthesis of Pb-BTC.

## 2.4. Analytical procedures

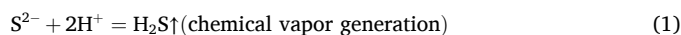
All water samples, beer samples and the CRM water sample (BWZ6676-2016C) were pretreated with 0.03 % (m/v) NaOH solution. The prepared Pb-BTC was stored at room temperature and weighed it when needed. Pb-BTC suspension was prepared by dispersing 60 mg of Pb-BTC in 1 mL of deionized water and shaking the solution before each used. Pb-BTC suspension was sucked by a plastic dropper and one drop of Pb-BTC suspension was dropped to the paper sheet. Pb-BTC was uniformly distributed on the paper with water was absorbed by the paper. The Pb-BTC fabricated test paper (wet) was used for further detection. The Pb-BTC test paper is disposable, so it needs to be replaced after use.

As illustrated in Scheme 1, the CVG-visual/smartphone RGB readout colorimetric system comprises a syringe, a headspace bottle (15 mL) and Pb-MOF fabricated chromatography paper (diameter: 1.5 cm). In the procedure, 10 mL sample solution or  $S^{2-}$  standard solution was added to the headspace vial, the Pb-MOF fabricated chromatography paper was placed in sealed cover before tightening sealing cap. Subsequently, 5 mL of 6 % (v/v)  $\text{H}_2\text{SO}_4$  solution was injected into the bottle to react with  $S^{2-}$  and immediately produce gaseous  $\text{H}_2\text{S}$ .  $\text{H}_2\text{S}$  was then reacted with Pb-BTC to form PbS, causing the color gradually changed from white to black. This color change can be observed both with naked-eye and smartphone.

## 3. Results and discussions

### 3.1. Mechanism discussions

Pb-BTC was prepared and utilized as a substrate for sensitive and selective detection of  $S^{2-}$  using the chemical vapor generation-colorimetric system.  $S^{2-}$  was converted to  $\text{H}_2\text{S}$  with the addition of  $\text{H}_2\text{SO}_4$  (chemical vapor generation process, Reaction 1). Subsequently,  $\text{H}_2\text{S}$  reacted with Pb-BTC, causing a change in the color of the paper sheet. The potential mechanism (Reaction 1 and Reaction 2) of the discoloration between Pb-BTC and  $\text{H}_2\text{S}$  was investigated through characterizations.



Pb-BTC before and after reaction were characterized by XRD and XRD data were presented in Fig. S1. The XRD peaks of Pb-BTC remained



basically unchanged after reaction, indicating no significant alteration in the crystal structure of Pb-BTC. However, three additional peaks were found after reaction, it matched well with the standard card of PbS (PDF#02-0699)(Tan et al., 2017), demonstrating the generation of PbS (Reaction 2). SEM characterization was used for further demonstrating this hypothesis. Pb-BTC exhibits a well-structured prismatic crystal morphology before the reaction (Fig. S3a-3b). After reacting with H<sub>2</sub>S, its surface became rougher (Fig. S3c-3d). With the increase of H<sub>2</sub>S concentration, the crystal structure was partially disrupted and even collapsed (Fig. S3e-3h). Energy-dispersive spectroscopy (EDS) indicated that uniform distribution of Pb and S on the Pb-BTC (Fig. 1a-1c), with sulfur observed in Pb-BTC after reaction (Table S1), further confirming the generation of PbS. The production of PbS was further elucidated by XPS. After reaction, the S 2p peaks appeared at 160.2 eV (2p<sub>3/2</sub>) and 161.4 eV (2p<sub>1/2</sub>), which attribute to the existence of S<sup>2-</sup> (Fig. 1e and Fig. S4c). Additionally, the binding energies of Pb 4f shifted from 138.2 eV and 143.1 eV (before reaction) to 137.3 eV and 142.2 eV (after reaction), respectively. In fine energy spectrum (Fig. S4b and S4d), peak of Pb-S was observed after reaction, further indicating the generation of PbS. (Cha et al., 2018; Lara et al., 2011).

### 3.2. Optimization of conditions

Different experimental parameters can influence the efficiency of H<sub>2</sub>S production, subsequently affecting the reaction of Pb-BTC with H<sub>2</sub>S. Therefore, Pb-BTC concentration, H<sub>2</sub>SO<sub>4</sub> concentration and reaction time were optimized. The V(R + G + B) value represents the summation of red value (R), green value (G) and blue value (B), expressed as V(R + G + B) = V<sub>R</sub> + V<sub>G</sub> + V<sub>B</sub>. A decrease in the V(R + G + B) value indicating darkening of the color.

The concentration of Pb-BTC plays a crucial role for the sensitivity of this system, so that Pb-BTC concentration was optimized. As depicted in Fig. 2a, as the Pb-BTC concentration increased, V(R + G + B) value gradually decreased and reached a plateau at 60 mg/mL, consistent with the results of visual method. Therefore, 60 mg/mL Pb-BTC was used in further experiments. H<sub>2</sub>SO<sub>4</sub> concentration significantly affects the production of H<sub>2</sub>S, as insufficient of H<sub>2</sub>SO<sub>4</sub> leads to incomplete conversion of S<sup>2-</sup> to H<sub>2</sub>S. Fig. 2b demonstrates that the optimal V(R + G + B) value was obtained at a H<sub>2</sub>SO<sub>4</sub> concentration of 6 % (v/v), corroborating results obtained with naked eye. Subsequently, reaction time was optimized to achieve stable results. The V(R + G + B) value decreased with time and stabilized at 10 min (Fig. 2c), so that 10 min was chosen for subsequent experiments. Furthermore, five types of test paper (Whatman grade 1 filter paper (test paper 1), Whatman grade 2 filter paper (test paper 2), Whatman grade 3 MM chromatography paper (test paper 3), Whatman grade 4 filter paper (test paper 4) and Whatman grade 5 filter paper (test paper 5)) were used for investigating the effect of test paper. Under optimized conditions, test paper 3 exhibits the best analytical performance both in visual mode and smartphone mode, so that test paper 3 was chosen for the subsequent experiments (Fig. S5). Comparison between an old test paper (stored at room temperature for 30 days) and a new test paper (stored at room temperature for 1 days) indicates minimal discrepancy in both smartphone readout mode and visual mode, affirming the stability of Pb-BTC at room temperature (Fig. 2d). Under optimal conditions, good reproducibility and stability (relative standard deviation (RSD) = 1.8 %) were achieved in both smartphone and naked-eye (Fig. S6 and Fig. S7).

In summary, the optimized conditions of this study can be outlined as follows: (1) Pb-BTC concentration: 60 mg/mL; (2) H<sub>2</sub>SO<sub>4</sub> concentration: 6 % (v/v); (3) reaction time: 10 min.

### 3.3. Interferences

The anti-interference capability stands as a pivotal factor for potential application of methodologies in real sample analysis. Hence, this section delves into interference tests. Fortunately, chemical vapor

generation (CVG) was used as a sampling method for this colorimetric system, offers notable advantages including high efficiency of vapor generation and efficient matrix separation.

Given the prevalence of organic compounds in beer samples, interference tests were conducted using this method with addition of organic compounds, including ethanol (Et), fructose (Fru), lactose (Lac), maltose (Mal), sucrose (Suc), glucose (Glu), tartaric acid (TA), oxalic acid (OA) and citric acid (CA). As illustrated in Fig. 3, these organic compounds do not interfere with the detection of S<sup>2-</sup>, even at a concentration (50 µg/mL) 50-fold higher than that of S<sup>2-</sup> (1 µg/mL). Visual colorimetry revealed no significant color change in the absence of S<sup>2-</sup>, indicating that co-existing substances do not affect the detection of S<sup>2-</sup>. Notably, a dark color is observed in the presence of S<sup>2-</sup>, maintaining consistency even when co-existing with organic compounds at high concentration (1 µg/mL S<sup>2-</sup> + 50 µg/mL co-existing organic compounds). Similar analytical results were obtained for smartphone RGB readout method, underscoring its favorable tolerance to interference. S<sup>2-</sup> exhibits a propensity to bind with most metal ions, forming insoluble or slightly soluble species, mitigating potential metal interferences in the environment. Various interference sources (K<sup>+</sup>, Na<sup>+</sup>, Cl<sup>-</sup>, I<sup>-</sup>, Br<sup>-</sup>, F<sup>-</sup>, CO<sub>3</sub><sup>2-</sup>, PO<sub>4</sub><sup>3-</sup>, NO<sub>3</sub><sup>-</sup>, CH<sub>3</sub>COO<sup>-</sup> (Ac<sup>-</sup>)) were examined. There is no doubt that these co-existing ions also have no effect on the determination of S<sup>2-</sup> (Fig. S8). These findings underscore the high potential application of the proposed method for H<sub>2</sub>S detection.

### 3.4. Sample analysis

Various concentrations of S<sup>2-</sup> standard solutions (0, 0.02, 0.05, 0.1, 0.2, 0.5, 1, 2, 5 and 10 µg/mL) were assessed using this method to evaluate its performance. As the concentration of S<sup>2-</sup> increased, the color of the test paper gradually changed from white to black (Fig. 4b). S<sup>2-</sup> at a concentration of 0.05 µg/mL could be detected using smartphone RGB readout method, while 0.2 µg/mL S<sup>2-</sup> can be readout by naked-eye (Fig. S9). Both concentrations meet the WHO-stated value (0.5 µg/mL) for water system. In addition, V(R + G + B) value decreased gradually with the increase of S<sup>2-</sup> concentration, displaying a strong linear relationship with S<sup>2-</sup> in the range of 0–2 µg/mL (Fig. 4a). The analytical performance of this system was in comparison with others (Table S2). The results show that this method presents a low detectable limit and a wide linear range. This method is not only a portable, low-cost and easy-to-operate method, but also a sensitive and selective analytical system for S<sup>2-</sup>.

For verifying the applicability and accuracy of this colorimetric system, three water samples and a CRM water sample (BWZ6676-2016C) were analyzed. As depicted in Fig. 4b, the colors were consistent with those of standard cards in visual mode, and satisfactory recoveries (102 %–111 %) were achieved using smartphone RGB readout mode, as summarized in Table 1. To further validate the accuracy of this method, the CRM water sample (BWZ6676-2016C) was measured 7 times to obtain an average value of 1.018 µg/mL (n = 7, f = 6), which is almost identical to the certified value (1 µg/mL). In addition, the value of s (standard deviation) was 0.030. The calculation of equation ( $t = \frac{\bar{x}-\mu}{s} \sqrt{n}$ ) yields 1.59, which is less than 2.45 in 95 % confidence level (t<sub>0.05, 6</sub> = 2.45), t-test demonstrated that the analytical result by this method had no significant difference with the certified value. Furthermore, this method was further applied to beer samples, their colors were matched well with the standard card (Fig. S10), and their corresponding results readout by smartphone were presented in Table 1, recoveries ranging from 97 % to 109 %. These results indicate the method's significant potential for on-site analysis of S<sup>2-</sup>.

## 4. Conclusions

A miniaturized chemical vapor generation-colorimetric analytical system was developed for the selective and sensitive detection of S<sup>2-</sup>. In

the process of chemical vapor generation,  $S^{2-}$  was transformed to  $H_2S$  and separated from the complicated matrix, so that the interferences from the matrix can be eliminated efficiently. The generated  $H_2S$  gas was then reacted with Pb-BTC, and PbS was formed on its surface and caused the Pb-BTC fabricated paper turned to black from white. The color changes were available to both smartphone readout mode and visual mode. The experimental conditions were optimized, and detectable limits of 0.05  $\mu\text{g/mL}$  and 0.2  $\mu\text{g/mL}$  were achieved under smartphone mode and visual mode, it is far below the stated value of WHO (0.5  $\mu\text{g/mL}$ ). Several real samples were measured by this colorimetric system to demonstrate its accuracy and applicability, including beer samples, water samples and a CRM water sample (BWZ6676-2016C). This method is a portable, low-cost and easy-to-operate analytical system for  $S^{2-}$  rapid and on-site analysis.

### CRedit authorship contribution statement

**Jihong Chen:** Writing – original draft, Investigation, Data curation, Conceptualization. **Qian Yao:** Writing – review & editing, Validation, Investigation, Funding acquisition. **Xiaoyu Dong:** Validation, Investigation. **Jiayuan Tang:** Validation, Investigation. **Shu Zhang:** Writing – review & editing, Conceptualization. **Yuyao Ji:** Writing – review & editing, Supervision, Methodology, Conceptualization. **Zhirong Zou:** Writing – review & editing, Supervision, Project administration, Funding acquisition, Conceptualization.

### Declaration of competing interest

The authors declare that they have no known competing financial interests or personal relationships that could have appeared to influence the work reported in this paper.

### Data availability

Data will be made available on request.

### Acknowledgements

This work was financially supported by the National Natural Science Foundation of China (No. 22106113), Sichuan Science & Technology Program (No. 2023NSFSC1112) and Opening Foundation from Key Laboratory of Low-cost Rural Environmental Treatment Technology at Sichuan Institute of Arts and Science, Education Department of Sichuan Province (No. XCH2023ZA-04).

### Appendix A. Supplementary data

Supplementary data to this article can be found online at <https://doi.org/10.1016/j.fochx.2024.101767>.

### References

- Baskoro, F., Wong, H. Q., Labasan, K. B., Cho, C.-W., Pao, C. W., Yang, P. Y., ... Yen, H. J. (2021). An efficient and reversible battery anode electrode derived from a lead-based metal-organic framework. *Energy & Fuels*, 35(11), 9669–9682. <https://doi.org/10.1021/acs.energyfuels.1c00517>
- Buragohain, A., & Biswas, S. (2016). Cerium-based azide- and nitro-functionalized UiO-66 frameworks as turn-on fluorescent probes for the sensing of hydrogen sulphide. *CrystEngComm*, 18(23), 4374–4381. <https://doi.org/10.1039/c6ce00032k>
- Campanella, B., & D'Ulivo, A. (2024). *Mechanisms of chemical vapor generation by aqueous boranes for trace element analysis*. Twenty years of investigations: Applied Spectroscopy Reviews. <https://doi.org/10.1080/05704928.2024.2328328>
- Cha, J. H., Kim, D. H., Choi, S. J., Koo, W. T., & Kim, I. D. (2018). Sub-parts-per-million hydrogen sulfide colorimetric sensor: Lead acetate anchored nanofibers toward halitosis diagnosis. *Analytical Chemistry*, 90(15), 8769–8775. <https://doi.org/10.1021/acs.analchem.8b01273>
- Chen, J., Wang, J., Peng, Y., Liu, F., Jia, M., Lai, Y., Li, J., & Jiang, L. (2021).  $\text{Bi}_2\text{O}_3$  nanostructure-based photoanodes for photoelectrochemical determination of trace soluble sulfides. *ACS Applied Nano Materials*, 4(6), 5778–5784. <https://doi.org/10.1021/acsanm.1c00592>

- Chen, Z., Li, L., Zhao, Z., Zhu, Y., & Liu, Z. (2024). Responsive luminescent silver-based metal-organic frameworks for highly sensitive and selective detection of hydrogen sulfide in biological system via a self-assembled headspace separation device. *Talanta*, 267, Article 125170. <https://doi.org/10.1016/j.talanta.2023.125170>
- Hall, J. R., & Schoenfish, M. H. (2018). Direct electrochemical sensing of hydrogen sulfide without sulfur poisoning. *Analytical Chemistry*, 90(8), 5194–5200. <https://doi.org/10.1021/acs.analchem.7b05421>
- Hu, J., Li, C., Zhen, Y., Chen, H., He, J., & Hou, X. (2022). Current advances of chemical vapor generation in non-tetrahydroborate media for analytical atomic spectrometry. *TrAC Trends in Analytical Chemistry*, 155, Article 116677. <https://doi.org/10.1016/j.trac.2022.116677>
- Hu, P., Wang, X., Wang, Z., Dai, R., Deng, W., Yu, H., & Huang, K. (2019). Recent developments of hydride generation in non-atomic spectrometric methods. *TrAC Trends in Analytical Chemistry*, 119, Article 115617. <https://doi.org/10.1016/j.trac.2019.07.028>
- Huang, K., Dai, R., Deng, W. Q., Guo, S. J., Deng, H., Wei, Y., ... Xiong, X. L. (2018). Gold nanoclusters immobilized paper for visual detection of zinc in whole blood and cells by coupling hydride generation with headspace solid phase extraction. *Sensors and Actuators B: Chemical*, 255, 1631–1639. <https://doi.org/10.1016/j.snb.2017.08.177>
- Jiang, C. X., Ye, S., Xiao, J., Tan, C., Yu, H. M., Xiong, X. L., ... Zou, Z. R. (2023). Hydride generation-smartphone RGB readout and visual colorimetric dual-mode system for the detection of inorganic arsenic in water samples and honeys. *Food Chemistry: X*, 18. <https://doi.org/10.1016/j.fochx.2023.100634>
- Lara, R. H., Briones, R., Monroy, M. G., Mullet, M., Humbert, B., Dossot, M., ... Cruz, R. (2011). Galena weathering under simulated calcareous soil conditions. *Science of the Total Environment*, 409(19), 3971–3979. <https://doi.org/10.1016/j.scitotenv.2011.06.055>
- Li, D. D., Qu, L. H., Hu, K., Long, Y. T., & Tian, H. (2015). Monitoring of endogenous hydrogen sulfide in living cells using surface-enhanced raman scattering. *Angewandte Chemie-International Edition*, 54(43), 12758–12761. <https://doi.org/10.1002/anie.201505025>
- Li, H. Y., Zhao, S. N., Zang, S. Q., & Li, J. (2020). Functional metal-organic frameworks as effective sensors of gases and volatile compounds. *Chemical Society Reviews*, 49(17), 6364–6401. <https://doi.org/10.1039/c9cs00778d>
- Li, L., Jiang, C., Xiao, J., Luo, H., Zhang, S., Zou, Z., & Huang, K. (2023). Applications of photochemical vapor generation-analytical atomic spectrometry for the speciation analysis of arsenic, mercury and selenium. *Spectrochimica Acta Part B: Atomic Spectroscopy*, 199, Article 106579. <https://doi.org/10.1016/j.sab.2022.106579>
- Lin, Y., Ye, S., Tian, J., Leng, A., Deng, Y., Zhang, J., & Zheng, C. (2023). Paper-assisted ratiometric fluorescent sensors for on-site sensing of sulfide based on the target-induced inner filter effect. *Journal of Hazardous Materials*, 459, Article 132201. <https://doi.org/10.1016/j.jhazmat.2023.132201>
- Liu, J. S., Bao, H. J., Ma, D. L., & Leung, C. H. (2019). Silver nanoclusters functionalized with Ce(III) ions are a viable “turn-on-off” fluorescent probe for sulfide. *Microchimica Acta*, 186(1), 16. <https://doi.org/10.1007/s00604-018-3149-z>
- Pan, Y., Fang, Z., Chen, H. J., Long, Z., & Hou, X. D. (2021). Visual detection of  $S^{2-}$  with a paper-based fluorescence sensor coated with CdTe quantum dots via headspace sampling. *Luminescence*, 36(6), 1525–1530. <https://doi.org/10.1002/bio.4097>
- Rajamanikandan, R., & Ilanchelian, M. (2022). Simple smartphone merged rapid colorimetric platform for the environmental monitoring of toxic sulfide ions by cysteine functionalized silver nanoparticles. *Microchemical Journal*, 174, Article 107071. <https://doi.org/10.1016/j.microc.2021.107071>
- Sadeghzadeh, H., & Morsali, A. (2010). Sonochemical synthesis and structural characterization of a nano-structure Pb(II) benzenetricarboxylate coordination polymer: New precursor to pure phase nanoparticles of Pb(II) oxide. *Journal of Coordination Chemistry*, 63(4), 713–720. <https://doi.org/10.1080/00958970903502736>
- So, H., Chae, J. B., & Kim, C. (2019). A thiol-containing colorimetric chemosensor for relay recognition of  $\text{Cu}^{2+}$  and  $S^{2-}$  in aqueous media with a low detection limit. *Inorganica Chimica Acta*, 492, 83–90. <https://doi.org/10.1016/j.ica.2019.04.024>
- Tan, L., Zhou, Y. F., Ren, F. Q., Benetti, D., Yang, F., Zhao, H. G., ... Ma, D. L. (2017). Ultrasmall PbS quantum dots: A facile and greener synthetic route and their high performance in luminescent solar concentrators. *Journal of Materials Chemistry A*, 5(21), 10250–10260. <https://doi.org/10.1039/c7ta01372h>
- Tang, S., Qi, T., Xia, D. S., Xu, M. C., Xu, M. Y., Zhu, A. N., ... Lee, H. K. (2019). Smartphone nanocolorimetric determination of hydrogen sulfide in biosamples after silver-gold core-shell nanoprisms-based headspace single-drop microextraction. *Analytical Chemistry*, 91(9), 5888–5895. <https://doi.org/10.1021/acs.analchem.9b00255>
- Tian, J., Tu, Q., Li, M., Zhao, L., Zhu, Y., Lee, J.-H., Gai, Z., Zhao, G., & Ma, Y. (2024). Development of fluorescent GO-AgNPs-Eu<sup>3+</sup> nanoparticles based paper visual sensor for foodborne spores detection. *Food Chemistry: X*, 21, Article 101069. <https://doi.org/10.1016/j.fochx.2023.101069>
- Tolessa, T., Tan, Z. Q., & Liu, J. F. (2018). Hydride generation coupled with thioglycolic acid coated gold nanoparticles as simple and sensitive headspace colorimetric assay for visual detection of Sb(III). *Analytica Chimica Acta*, 1004, 67–73. <https://doi.org/10.1016/j.aca.2017.11.073>
- Wang, H., Wang, J. L., Yang, S. X., Tian, H. Y., Liu, Y. G., & Sun, B. G. (2018). Highly selective and rapidly responsive fluorescent probe for hydrogen sulfide detection in wine. *Food Chemistry*, 257, 150–154. <https://doi.org/10.1016/j.foodchem.2018.02.130>
- Wu, P., He, L. A., Zheng, C. B., Hou, X. D., & Sturgeon, R. E. (2010). Applications of chemical vapor generation in non-tetrahydroborate media to analytical atomic spectrometry. *Journal of Analytical Atomic Spectrometry*, 25(8), 1217–1246. <https://doi.org/10.1039/c003483e>

- Xiong, J., Xu, K. L., Hou, X. D., & Wu, P. (2019). AuNCs-catalyzed hydrogen selenide oxidation: Mechanism and application for headspace fluorescent detection of se(IV). *Analytical Chemistry*, 91(9), 6141–6148. <https://doi.org/10.1021/acs.analchem.9b00738>
- Yang, Z., Zhang, W., Yin, Y., Fang, W., & Xue, H. (2022). Metal-organic framework-based sensors for the detection of toxins and foodborne pathogens. *Food Control*, 133, Article 108684. <https://doi.org/10.1016/j.foodcont.2021.108684>
- Yin, C., Liu, T., Wu, M., Liu, H., Sun, Q., Sun, X., Niu, N., & Chen, L. (2022). Smartphone-integrated dual-emission fluorescence sensing platform based on carbon dots and aluminum ions-triggered aggregation-induced emission of copper nanoclusters for on-site visual detecting sulfur ions. *Analytica Chimica Acta*, 1232, Article 340460. <https://doi.org/10.1016/j.aca.2022.340460>
- Yuan, P., Deng, Z., Qiu, P., Yin, Z., Bai, Y., Su, Z., & He, J. (2023). Bimetallic metal-organic framework nanorods with peroxidase mimicking activity for selective colorimetric detection of salmonella typhimurium in food. *Food Control*, 144, Article 109357. <https://doi.org/10.1016/j.foodcont.2022.109357>
- Yuan, X., Zhang, J., Yang, H., Yang, Q., Li, L., Zhang, M., & Huang, K. (2022). Quantum dots immobilized paper for specific and sensitive quantitation of Ni(II) by headspace photochemical vapor generation: Mechanism and application for RGB detection in tea fusion with a smartphone. *Sensors and Actuators B: Chemical*, 372, Article 132686. <https://doi.org/10.1016/j.snb.2022.132686>
- Zhang, C. Y., Wang, B., Li, W. B., Huang, S. Q., Kong, L., Li, Z. C., & Li, L. (2017). Conversion of invisible metal-organic frameworks to luminescent perovskite nanocrystals for confidential information encryption and decryption. *Nature Communications*, 8, 1138. <https://doi.org/10.1038/s41467-017-01248-2>
- Zhang, M. Z., Deng, M. J., Ma, J. S., & Wang, X. Q. (2014). An evaluation of acute hydrogen sulfide poisoning in rats through serum metabolomics based on gas chromatography-mass spectrometry. *Chemical & Pharmaceutical Bulletin*, 62(6), 505–507. <https://doi.org/10.1248/cpb.c13-00988>
- Zhang, Y., Hu, K., Yuan, B., Zhu, X., Chen, X., & Huang, K. (2023). Gasoline residue-prepared carbon dots embedded metal-organic frameworks for selective and sensitive detection of sulfide ions. *Microchemical Journal*, 193, Article 109035. <https://doi.org/10.1016/j.microc.2023.109035>
- Zou, Z., Jiang, X., Li, L., Yao, Q., Luo, H., & Huang, K. (2020). Photochemical vapor generation of selenium: Mechanisms and applications. *Trends in Environmental Analytical Chemistry*, 27, Article e00094. <https://doi.org/10.1016/j.teac.2020.e00094>
- Zou, Z. R., Hu, J., Xu, F. J., Hou, X. D., & Jiang, X. M. (2019). Nanomaterials for photochemical vapor generation-analytical atomic spectrometry. *TrAC-Trends in Analytical Chemistry*, 114, 242–250. <https://doi.org/10.1016/j.trac.2019.03.012>
- Zou, Z. R., Ye, S., Xiao, J., Jiang, C. X., Zhang, S., Tan, C., ... Huang, K. (2023). Ag-containing metal organic framework reacted with AsH<sub>3</sub>: Mechanism and application for inorganic arsenic detection by hydride generation-smartphone RGB readout colorimetric system. *Food Chemistry*, 428, Article 136806. <https://doi.org/10.1016/j.foodchem.2023.136806>